Cellulose (2023) 30:4263–4276
https://doi.org/10.1007/s10570-023-05138-3

ORIGINAL RESEARCH

# Adjuvant action of needle-shaped BC microfibrils

**Özge Süer · Aytül Gül · Elif Esin Hameş**

Received: 18 September 2022 / Accepted: 5 March 2023 / Published online: 30 March 2023


**Abstract** Bacterial cellulose (BC) is an unbranched biopolymer produced by microorganisms and composed of glucopyranose units linked by β-1,4 bonds. This study investigates the adjuvant action of needle-shaped BC microfibrils (BCmFs) in vitro using bovine serum albumin (BSA) as a model antigen. BC produced by the static culture of *Komagataibacter xylinus* was then microparticled (1–5 µm) by acid hydrolysis and characterized using Dynamic Light Scattering and Scanning Electron Microscopy. Subsequently, Attenuated Total Reflectance-Fourier-Transform Infrared Spectroscopy, cytotoxicity, TNF-α (tumour necrosis factor-alpha) and IL-6 (interleukin-6) cytokine secretion, and cellular uptake of the BCmFs-BSA conjugate on the human monocyte cell line (U937) differentiated into macrophages were performed. The microfibrils were determined to be 1–5 µm in size, needle-shaped, with a zeta potential of −32 mV. Their conjugation with the model antigen, BSA, was demonstrated by FTIR analysis. In the cytotoxicity assay, BCmFs-BSA in macrophage cells showed high viability (over 70%). Although the highest TNF-α cytokine level (113 pg/ml) was obtained with BCmFs-BSA (Bovine serum albumin) conjugate (500 µg/ml) and was statistically significant ($p = 0.0001$) compared to the positive control group (BSA-aluminium hydroxide), IL-6 cytokine levels were not statistically different from those in the control group as desired. It has been shown in macrophage-differentiated U937 cells that microbially synthesized BC in the form of needle-shaped microfibrils (BCmFs) has a high cellular uptake capacity and increases the immunogenicity of the antigen. These results demonstrate for the first time that BCmFs have the potential to serve as a vaccine adjuvant.

**Keywords** Bacterial cellulose · Needle-shaped microfibrils · *Komagataibacter xylinus* · Vaccine · Adjuvant

Ö. Süer · A. Gül · E. E. Hameş
Department of Bioengineering, Graduate School of Natural and Applied Sciences, Ege University, Izmir, Türkiye

Ö. Süer
Department of Food Engineering, Faculty of Engineering, Izmir University of Economics, Izmir, Türkiye

E. E. Hameş (✉)
Department of Bioengineering, Faculty of Engineering, Ege University, 35100 Bornova, Izmir, Türkiye
e-mail: esin.hames@ege.edu.tr

## Introduction

As an alternative to live vaccines, inactivated or subunit vaccines produced from microorganisms or recombinant antigens are safer due to their inability to cause antigenic proliferation in the host. However, they induce weak immune responses (Plotkin 2014). Therefore, these vaccines need adjuvants, that help

induce strong and long-term antigen-specific immune responses (Zhang et al. 2015).

Adjuvants are compounds that increase the specific immune response to the target antigen. Although they were discovered 100 years ago, aluminium salts (alum) are still the most widely used adjuvant today (Del Giudice et al. 2018; Nanishi et al. 2020). However, alum adjuvants have serious side effects that cause local pain and inflammation at the injection site, causing granulomas, inducing IgE (immunoglobulin E) production, causing a tendency to allergy, and potentially leading to neurotoxicity (Aguilar and Rodríguez 2007). Freund's adjuvant, developed as an alternative to aluminium salts, has extreme adjuvant activity and but is unsuitable for humans because of the risk of inducing severe local reactions (Del Giudice et al. 2018; Wang et al. 2010). In addition to these adjuvants, particulate systems are another approach to enhancing the immunogenicity of an antigen. Particulate adjuvants (liposomes, virosomes, polymers, emulsions, etc.) can act as an antigen delivery system by protecting antigens from premature degradation by cellular enzymes and inducing cellular uptake and targeting of antigens by antigen-presenting cells (APCs) (Kalam et al. 2017). Alternatively, adjuvants can also consist of a combination of multiple substances. For example, MF59 is a licensed adjuvant with an oil-in-water emulsion system composed of squalene surrounded by a monolayer of non-ionic detergents (Calabro et al. 2013). Therefore, there is still a need to develop effective and safe new adjuvants to increase recombinant sub-unit antigens' immunogenicity.

Biopolymers have recently been studied as carriers and/or adjuvants due to their biocompatibility, cost-effective production, modifiability, and ability to increase immunogenicity when conjugated with antigenic molecules (Mustafaev 2004). Bacterial cellulose (BC), synthesized by microorganisms, has the same chemical formula as plant-based cellulose, but it differs with nanofiber structure and various properties. Although many studies have been conducted to use BC as a skin replacement (Keskin et al. 2017), an artificial vessel (Oz et al. 2021), a scaffold for bone tissue engineering (Bilgi et al. 2016), a burn and wound dressing (Yang et al. 2010), and a drug delivery system (Mohd Amin et al. 2014; Müller et al. 2011) in the medical field, there is no study on its use as a vaccine adjuvant.

BC is a polymer known for its biocompatibility and is used in medical research. In addition, since BC is insoluble in water and takes the form of a network of nanofibers, needle-shaped microfibrils can be produced by hydrolysis. On the other hand, effective cellular uptake of needle-shaped particles has been reported. In light of this information, this study is based on the hypothesis that biocompatible, water-insoluble, and needle-shaped BC microfibrils will effectively stimulate the immune system against the antigen to which they are conjugated. This study aimed to compare BCmFs as an alternative vaccine adjuvant to aluminium salts (aluminium hydroxide and aluminium phosphate salts).

## Materials and methods

### Materials

Sodium hydroxide (NaOH), Bradford reagent, glucose, disodium hydrogen phosphate ($Na_2HPO_4$), yeast extract, citric acid ($C_6H_8O_7.H_2O$), methanol, and acetone were purchased from Merck KGaA Germany. Bacto peptone was from Lab M (MC024, UK); Gentamicin was purchased from Biochrom, UK. Bovine serum albumin (BSA), Fetal bovine serum (FBS), L-glutamine, tween 20®, 3-(4,5-dimethylthiazol-2-yl)-2, 5-diphenyl- tetrazolium bromide (MTT), Dimethyl sulfoxide (DMSO), trypan blue, sulfuric acid ($H_2SO_4$), Phorbol myristate acetate (PMA), ethanol, lipopolysaccharide (*Escherichia coli* LPS25), fluorescein isothiocyanate-conjugated bovine serum albumin (FITC-BSA) [A-9771] were from Sigma Chemicals, USA. A syringe filter (0.22 µm) was provided from Sartorius, France. RPMI 1640 medium, phosphate buffer saline (PBS), human TNF-α and human IL-6 ELISA kit, and Imject™ alum adjuvant were purchased from Thermo Fisher Scientific, USA., DAPI (6-diamidino-2-phenylindole) Fluoromount – G (SouthernBiotech, 0100–20).

### BC production

*Komagataibacter xylinus* (ATCC 700178) was used for the production of BC. Bacteria from the stock culture (− 20 °C) were inoculated into 10 ml of Hestrin and Schramm (HS) medium (glucose 20 g, $Na_2HPO_4$ 2.7 gr, bacto peptone 5gr, yeast extract 5

gr, citric acid 1.15 g and 1 L distilled water) (Hestrin and Schramm 1954) and incubated at 30 °C for 48 h. Then the active culture was transferred to 50 ml HS medium (2% v/v) and incubated at 30 °C, 150 rpm for 48 h. Pellets were used as inoculum (2% v/v) for BC production (50 ml of HS in 250 ml flasks) in the static culture at 30 °C for 7 days.

After incubation, the harvested BC membranes (Fig. 1) were boiled in 0.1 M NaOH alkaline solution at 90 °C for 1 h to remove nutrients and microbial cell debris. This process was repeated three times using fresh NaOH solution each time. Finally, BC membranes, which were then boiled three times with distilled water for 1 h, were autoclaved and stored at 4 °C until use (Keskin et al. 2017).

## Preparation of needle-shaped BCmFs

The hydrolysis process has been optimized to obtain BC microfibrils with homogeneous micrometre size distribution. Variables of 2.5–5 M sulfuric acid, 30–90 °C, and 120–240 min were used in the optimization, and the best results were obtained at 2.5 M sulfuric acid, 90 °C, and 210 min (data not shown).

BC membranes were cut into small pieces (1 cm × 1 cm), disintegrated in a mixer for a minute and filtered to remove excess water. Then, it was lyophilized at − 50 °C under a vacuum of 0.042 mbar for 24 h. The BC pieces adhered to each other were roughly divided into small pieces again and taken into 2.5 M sulfuric acid (3–4 g BC/L acid). It was treated at 90 °C with continuous stirring for 210 min. Finally, BCmFs that had become a white precipitate were neutralized by 5–6 cycles of centrifugation (15,000 g, 20 min) and washing with ultra-pure water.

## Characterization of BCmFs

Dynamic light scattering (DLS) (Zeta sizer Malvern-Nano-ZS, Malvern Instruments Ltd., UK) analysis was performed at 25 °C to determine the particle size and distribution and Zeta potential of the needle-shaped microfibrils. Samples were dispersed in ultrapure water and analysed in duplicate.

ATR-FTIR analysis of freeze-dried BCmFs and BCmFs-BSA conjugates were obtained with the PerkinElmer Spectrum Two FTIR spectrometer between the 4000 $cm^{-1}$ and 650 $cm^{-1}$ spectrum.

The dimensions and morphologies of the BC microfibrils were analysed using Scanning Electron Microscope (SEM, Jeol-JSM 6060, and Philips XL 30S FEG) after their surfaces were coated with 8 nm gold–palladium.

## Preparation of BCmFs-BSA conjugates

BSA was used as a model antigen (Kanchan and Panda 2007) to examine the adjuvant action of BCmFs. The adjuvant and antigen were conjugated by a simple mixing method. The amount of absorbed antigen was determined with the Bradford protein assay (Bradford 1976). For this, BCmFs sterilized by autoclaving in a UPS were centrifuged at 15,000 g for 20 min to remove the water and portioned into 24 well plates as 5 mg under aseptic conditions. Then, filter-sterilized BSA prepared at different concentrations (5000, 2500, 1000, 500, 250 and 100 mg/ml) in phosphate-buffered saline solution (pH 7.2) was added (1 ml) to the BCmFs samples (5 mg) (Devy et al. 2006).

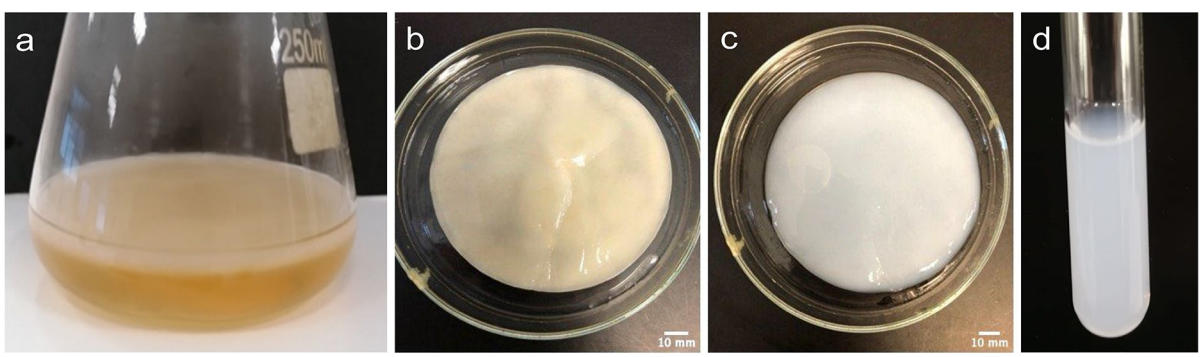


**Fig. 1** **a** BC production in static culture, **b** BC membrane, **c** purified BC membrane, **d** colloidal BC solution

Samples in the well plate were shaken at 37 °C for 48 h at 230 rpm for conjugation, then centrifuged (15,000 g for 20 min), and the supernatant was used for total protein assay. For this, 10 µl of supernatants were transferred to a new 96-well plate, 200 µl of Bradford's reagent was added, and spectrophotometric absorbance was measured at 595 nm after being kept in the dark for 10 min (Bradford 1976). The amount of unbound BSA in the supernatant was calculated using the BSA standard curve and subtracted from the initial BSA concentration to determine the amount of BSA in the conjugates. The BSA loading capacity (LC) of BCmFs suspended in BSA solution at different concentrations was calculated by the following Eq. (1)

$$LC = [Loaded\,BSA / Weight\,BCmfs] \times 100 \quad (1)$$

## Cytotoxicity and adjuvant activity of BCmFs

### *U937 cells differentiation into macrophage*

Differentiation of U937 human monocytes to macrophage was performed according to Debelec-Butuner et al. (2014) with slight modifications. The U937 cells were cultured in RPMI 1640 medium supplemented with 10% double inactivated FBS (fetal bovine serum), 1% L-glutamine, and %0.1 gentamicin (complete medium) at 37 °C with 5% $CO_2$. Cells were rested in a 96-well plate and a four-well chamber slide for one h prior to treatment, with an initial density of $5 \times 10^4$ and $5 \times 10^5$ cells per well, respectively. Hemocytometer measurements determined the cell concentration.

Cells were incubated for 20 h for macrophage differentiation by adding phorbol 12-myristate 13-acetate (PMA) at a final concentration of 16 nM. Adherent cell clumps were observed under the light microscope as an indicator of differentiation (Zeiss, Axio Vert.A1, Germany). At the end of the incubation, the cells were washed twice with RPMI 1640 (200 µl) and rested for 5 h at 37 °C, 5% $CO_2$, with the addition of a nutrient medium before treatment.

### *Cytotoxicity of BCmFs*

The in vitro cytotoxicity of BCmFs and their BSA conjugates (BCmFs-BSA) was determined by the MTT [(4,5-dimethylthiazol-2-yl)-2,5-diphenyltetrazolium bromide] assay (Mosmann 1983) on the macrophage differentiated U937 cells. Cells were incubated for 24 h with BCmFs-BSA, alum-BSA, and BCmFs in 96-well plates. Dimethyl sulfoxide (DMSO) (50% v/v) was used as a positive control, and the growth medium as a negative control. At the end of the incubation, the medium was removed, and 100 µl of serum-free RPMI 1640 containing %2 (0.5 mg/mL) MTT solution was added to each well. Next, the cells were incubated for 3 h at 37 °C in 5% $CO_2$. The medium was removed, and DMSO (100 µl) was added to each well to dissolve the formazan salts. After shaking the plate for 2 min at 400 rpm in the dark, absorbance (Versamax Microplate Reader, VWR, USA) was measured at 570 nm.

### *Cytokine release*

BSA (250 and 500 µg/ml), BCmFs-BSA (250 and 500 µg/ml), alum-BSA (250 and 500 µg/ml), BCmFs (5 mg/ml), alum (5 mg/ml), and lipopolysaccharide (LPS) (10 ng/ml) as a positive control were added to the macrophage cells, which were rested for 5 h after differentiation and incubated for 24 h. The macrophage cells were treated with only medium as a negative control (NC) for 24 h. After the treatment, the supernatant (conditioned medium-CM) was collected from the wells and centrifuged at 1400 rpm for a minute. The amounts of TNF-α and IL-6 cytokines present in CM were determined according to the manufacturer's instructions using human TNF-α and IL-6 ELISA kits with detection limits of 1.7 pg/ml and 2 pg/ml, respectively.

### *Cellular uptake*

In vitro cellular uptake was carried out using FITC-BSA-conjugated BCmFs in macrophage-differentiated U937 cell lines on four-well glass chamber slides (Niikura et al. 2013). Macrophage differentiated U937 cells were incubated with BCmFs-BSA-FITC (250 and 500 µg/ml) and as control with BSA-FITC (500 µg/ml), BCmFs, and medium. After incubation, cells were washed three times with PBS, incubated with methanol for 5 min and then with acetone for 30 s for fixation. The sample was dried at room temperature and stained with DAPI Fluoromount-G (6-diamidino-2-phenylindole) for 90 min at 37 °C,

then observed using a Confocal Laser Scanning Microscope (CLSM) (Zeiss LSM 880, Germany). CLSM images were obtained by scanning contrasting double-labelled specimens using a Zeiss Confocal LSM880 microscope equipped with an Argon-Krypton laser (Carl Zeiss Micro-imaging, Inc., NY, USA). Images captured with DAPI and FITC were overlaid to determine the localization and co-localization of fluorescent microparticles and cells.

### Statistical analysis

The data were processed using GraphPad Prism 9 (GraphPad Software Inc., USA). The statistical significance was estimated with a one-way unpaired analysis of variance (ANOVA). A $p$ value $< 0.05$ was considered statistically significant.

## Results

### Production and characterization of BCmFs

BC membranes produced in the H&S medium were cut into small pieces after cleaning, and BCmFs were obtained as a white precipitate via acid hydrolysis. The hydrogel-like native BC (Fig. 1a–c) was transformed into a colloidal form in ultrapure water after hydrolysis (Fig. 1d).

### Size distribution and Zeta potential analysis

DLS analysis is used to obtain information about particle size in spherical particles by relating the diffusion coefficient to the particle size through the Stokes–Einstein equation. Although the technique provides accurate and precise data on monodisperse spheres, for particles with a size of 3:1 and above, particle size analysis from the peak values in the graph can give more accurate results (Provder 1997). By DLS analysis, BCmFs were determined to be 1 µm (69%) and 5 µm (15%), and the polydispersity index (PdI) was 0.489. The particle size distribution of BCmFs is shown in Fig. 2.

The zeta potential is a physicochemical parameter that shows the stability of the material in the liquid. High positive or negative Zeta potential values cause large repulsive forces, causing particles with similar electrical charges to repel each other, thus preventing aggregation (Lunardi et al. 2021). In the case of stabilization, a minimum of 30 mV is required. Therefore, the zeta potential of BCmFs measured as -32 mV indicates stability.

### SEM analysis

With the hydrolysis process, it is seen that the fiber network structure (Fig. 3a) of the native BC is disrupted, and needle-shaped microfibrils are formed (Fig. 3b, c). One hundred microfibrils were measured from three SEM images with the ImageJ program, and it was determined that 78% of the microfibrils were 1.35–2.5 µm in length. BCmFs size distribution was also presented in the histogram (Fig. 3d).

### Preparation of BCmFs-BSA conjugates and FTIR analysis

Conjugates prepared using different concentrations of BSA were removed by centrifugation from the

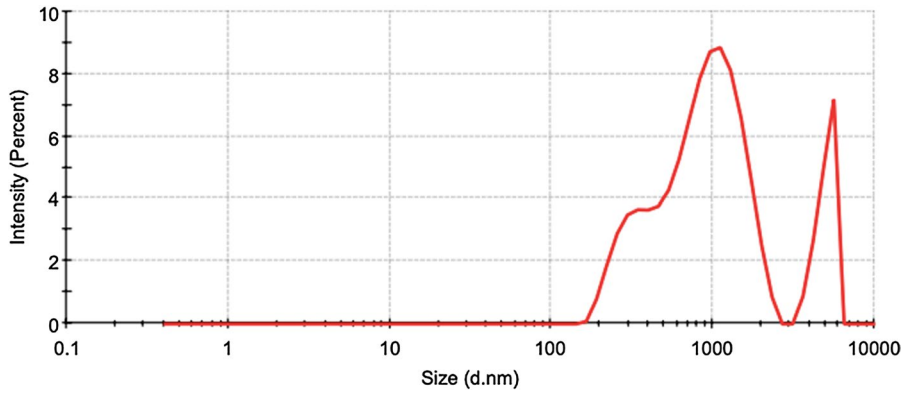


**Fig. 2** Size distribution of BCmFs

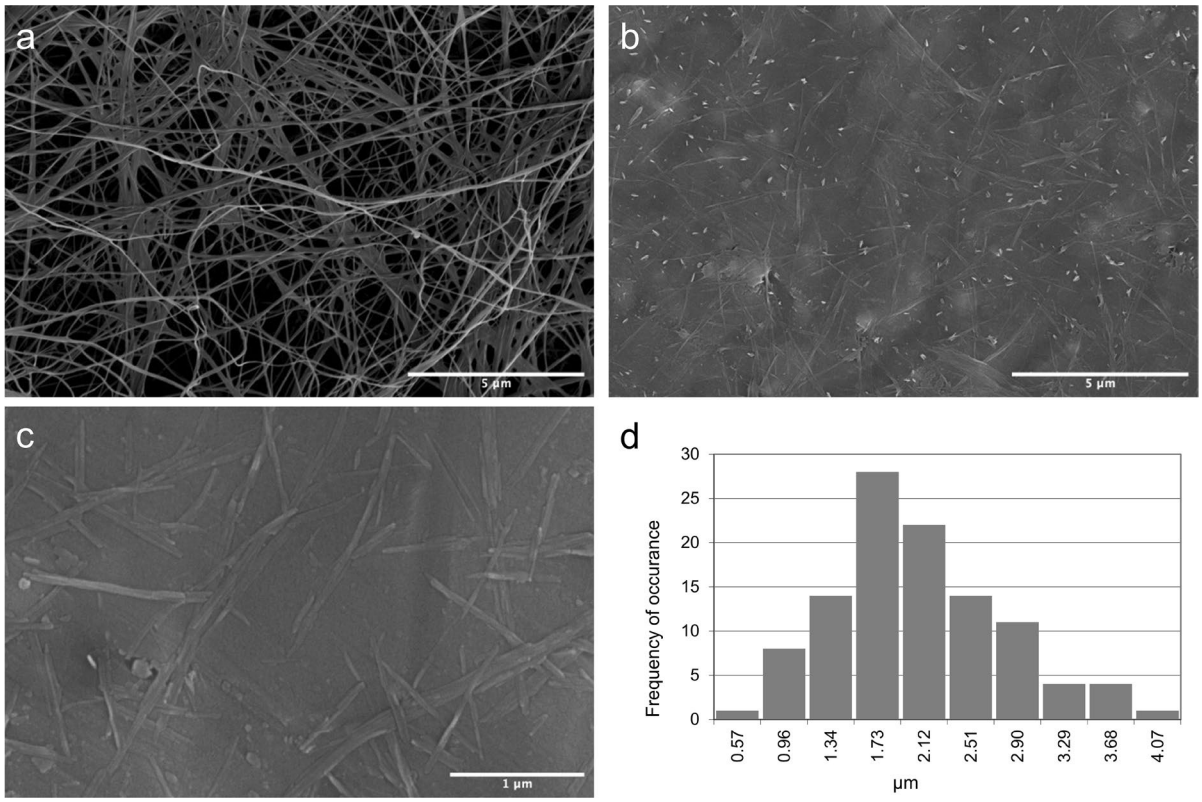


**Fig. 3** **a** SEM image of native BC at 25,000 magnifications, **b**, **c** SEM images of BCmFs at 25 and 200 thousand magnifications, **d** Size distribution histogram of BCmFs (Histogram template, Excel, American Society for Quality)

solution. The BSA loading capacity of BCmFs was determined as 79.5% by measuring the total protein amount in the remaining solution. The conjugate was prepared with 5 mg/ml BSA and 5 mg BCmFs.

FTIR spectrums showing the presence of BSA in BCmFs-BSA conjugates are presented in Fig. 4. The data were processed using OriginPro 2022b Learning Edition (Originlab Corporation, Northampton, Massachusetts, USA). The spectrum of BCmFs, BCmFs-BSA conjugate and BSA showed typical hydrogen bonds in 3600-3000 $cm^{-1}$, indicating N–H and O–H functional groups. In the BCmFs-BSA conjugate and BSA spectrums, the amide I and amide II bands specific to proteins appeared at 1654 $cm^{-1}$ and 1540 $cm^{-1}$, respectively. Both BC and BC/BSA conjugate samples showed the signals at 1050–1075 $cm^{-1}$, which indicate secondary alcohols and ether functions and are associated with the C–O– group in the cellulose chain backbone.

## Biocompatibility of BCmFs-BSA

The biocompatibility of BCmFs-BSA conjugates was determined by MTT assay on macrophage-differentiated U937 monocyte cells. In addition, PMA was used to differentiate monocyte cells into macrophages, and adherent cell clusters were observed (Fig. 5).

There was no statistically significant difference in cell viability of BCmFs-BSA conjugates obtained with two BSA concentrations (250 and 500 µg/ml) ($p = 0.9998$). BCmFs (75.59%) had lower cell viability than alum (98.44%) ($p < 0.0001$). Similarly, the cell viability of the BCmFs-BSA conjugate (500 µg/ml BSA) (74.7%) is lower than that of the Alum-BSA conjugate (500 µg/ml BSA) (86.2%) and BSA (500 µg/ml) (117.70%) (Respectively; $p = 0.0045$, $p < 0.0001$). Although the cell viability of BCmFs-BSA conjugates is lower than control groups, their viability percentage is over 70 (Fig. 6).

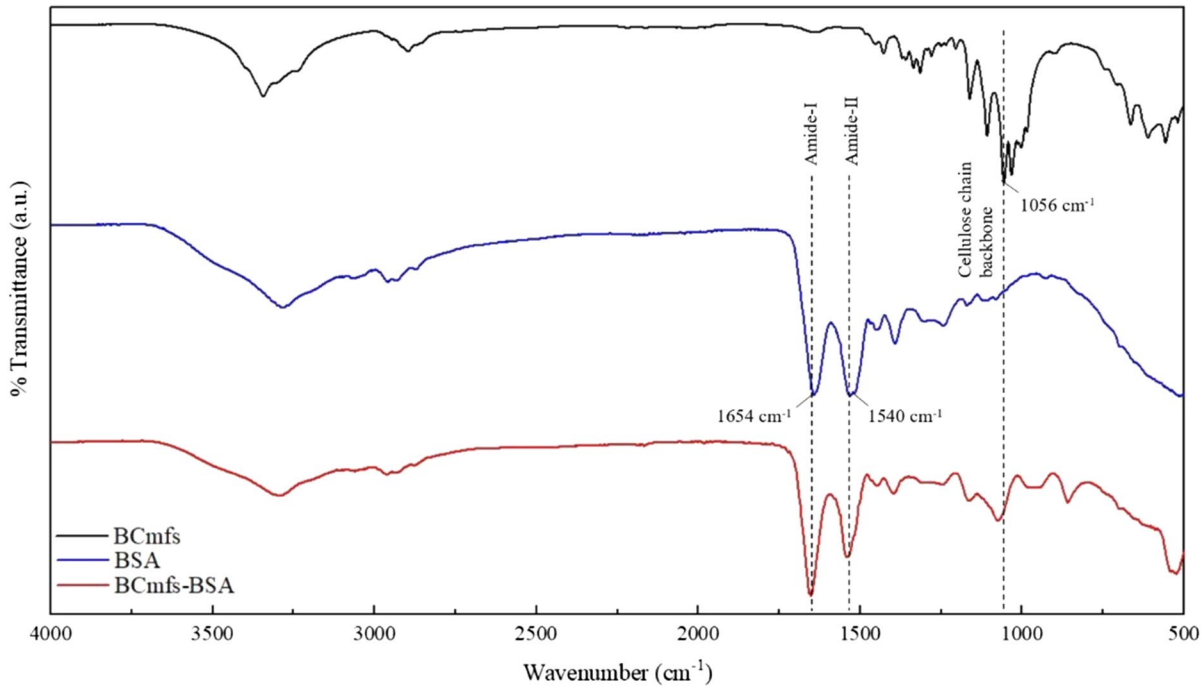


**Fig. 4** FTIR spectrum of BCmFs, BSA and conjugate of BCmFs-BSA

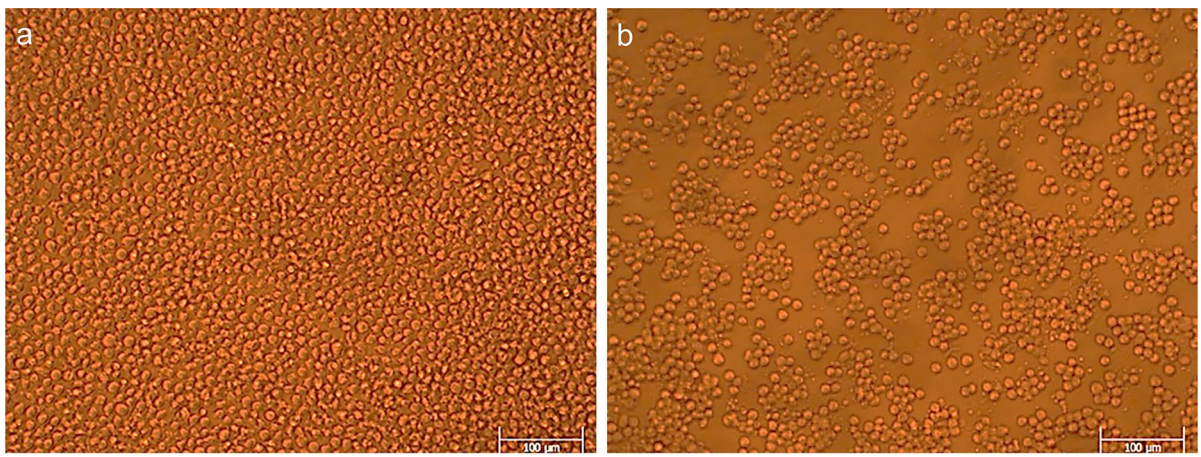


**Fig. 5** **a** U937 monocyte cells, **b** macrophage cells after differentiation of U937 monocyte cells by PMA stimulation (light microscope at 20X magnification)

The threshold value is 70% according to the ISO 10993–5:2009 standard and the results show that needle-shaped microfibril BC and its conjugates are not toxic to eukaryotic cells.

Cytokine release

The difference in TNF-α concentration between the undifferentiated cells (U937 monocyte cells) and

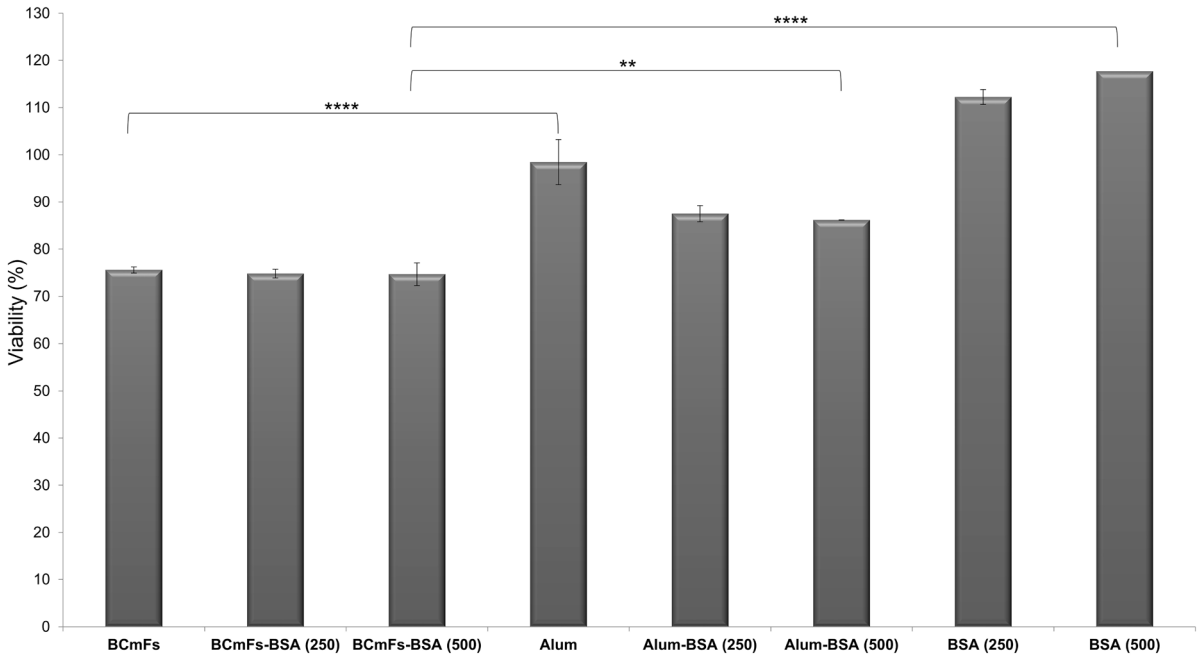


**Fig. 6** MTT results for cytotoxicity test (*$p < 0.05$; ****$p < 0.0001$)

the negative control showed that the cells were differentiated into macrophages (*$p = 0.0129$). There was no statistically significant difference between BCmFs and negative control groups ($p > 0.9999$). This result indicates that BCmFs did not induce cells and did not induce any immune response. There was no statistically significant difference between the BCmFs and alum groups ($p = 0.9936$). Alum and BCmFs showed similar TNF-α level when used alone. TNF-α induced by BSA (500 µg/ml) was 39 pg/ml, but when conjugated with BCmFs, the concentration increased to 114.3 pg/ml. In other words, the TNF-α level of the BCmFs-BSA (500 µg/ml) conjugate was measured 3.7 times higher than BCmFs and 2.9 times higher than BSA (500 µg/ml) (****$p < 0.0001$). The TNF-α levels were 2.18 times higher in the BCmFs-BSA (500 µg/ml) conjugate than in the BCmFs-BSA (250 µg/ml) conjugate (****$p < 0.0001$). The TNF-α levels in the BCmFs-BSA (500 µg/ml) conjugate were 1.78 times higher than in the Alum-BSA (500 µg/ml) conjugate (***$p = 0.0001$) (Fig. 7a). There was no statistically significant difference between all sample groups in IL-6 cytokine levels as desired (Fig. 7b).

Cellular uptake

Confocal microscopy was used to determine the cellular uptake of BCmFs-BSA-FITC. Successful cellular uptake was demonstrated in U937 macrophage cells treated with BCmFs-BSA-FITC for 24 h, and BCmFs-BSA-FITC was located outside the nucleus (Fig. 8). The difference in fluorescence intensity of BCmFs-BSA-FITC and BSA-FITC also supported the increased cellular uptake in the presence of BCmFs.

## Discussion

Vaccination is the most effective way to prevent and control diseases. The safety of vaccines has increased with recombinant vaccine technology, but these vaccines generally show weak immunogenic properties (Mchugh et al. 2015; Petrovsky and Aguilar 2004). Although it has been studied for years to administer weak immunogen vaccines in a single dose, it has yet to be advanced. Therefore, vaccine adjuvants used to increase the immunogenicity of the antigen

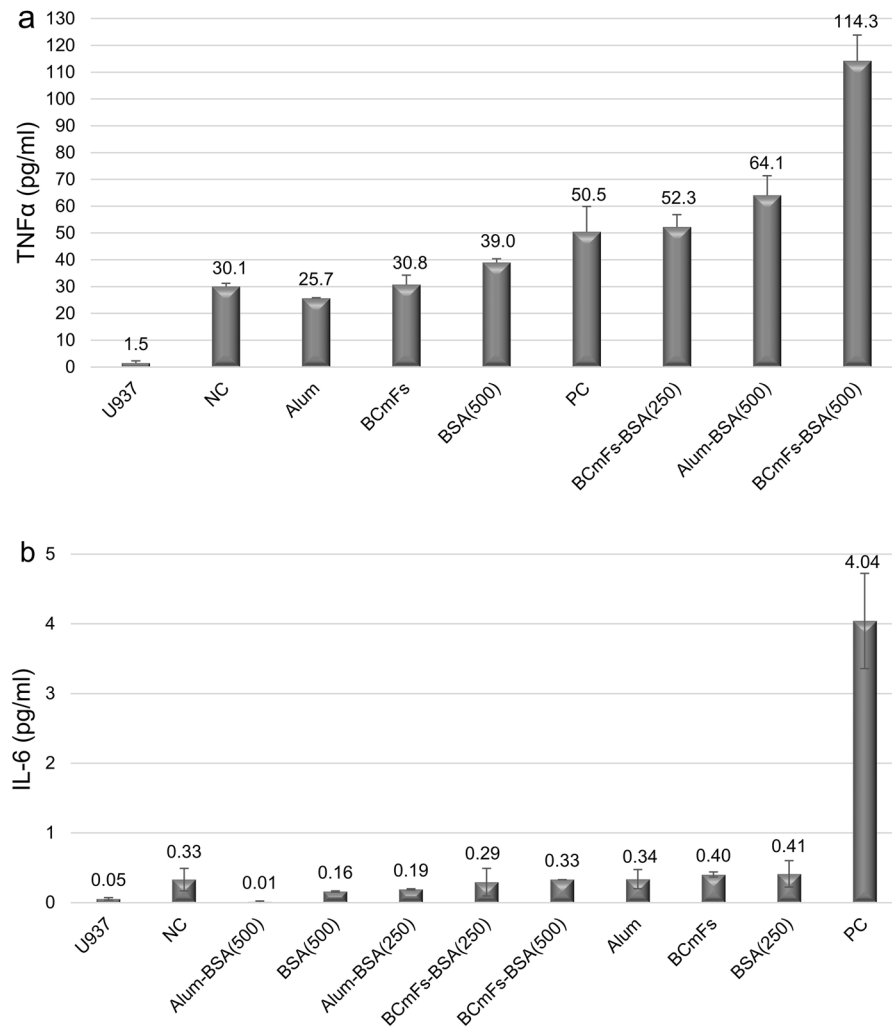


**Fig. 7** Cytokine release **a** TNF-α, **b** IL-6 (*NC* negative control, *PC* positive control)

have gained importance again, especially during the COVID-19 pandemic.

It is known that the polymers in the vaccine formulation are known to increase stability by binding to the antigens and acting as both carriers and adjuvants (Mustafaev 2004). Many plant and microbial polysaccharides have been investigated for their adjuvant potential. Various dextran derivatives have been shown to have immunological properties (Bauer et al. 2010). It has been reported that lentinan increases macrophage activity against the influenza virus and simultaneously induces cytokine production and cytotoxic T cell production (Vannucci et al. 2017). The adjuvant potency of different inulin isoforms has been reported both in vitro and in female Balb/c mice. It has been stated that delta inulin is the most immunologically effective derivative in activating the complement system, regulating chemokine production and cell surface protein expression by binding to monocytes. It has been reported to convert to potent immune adjuvant activity that enhances humoral and cellular responses to antigens (Cooper and Petrovsky 2011). In addition, among the biopolymers, mannan (Sheng et al. 2006), chitosan (Vasiliev 2014), and poly(γ-glutamic acid) (Seth et al. 2015) are reported to have adjuvant potential as alternatives to aluminium salts.

In this study, the adjuvant potential of the microfibrillar structure of BC, which has unique properties such as biocompatibility, high purity, and physical and chemical stability, was investigated (Keskin et al. 2017; Pertile et al. 2010; Piatkowski

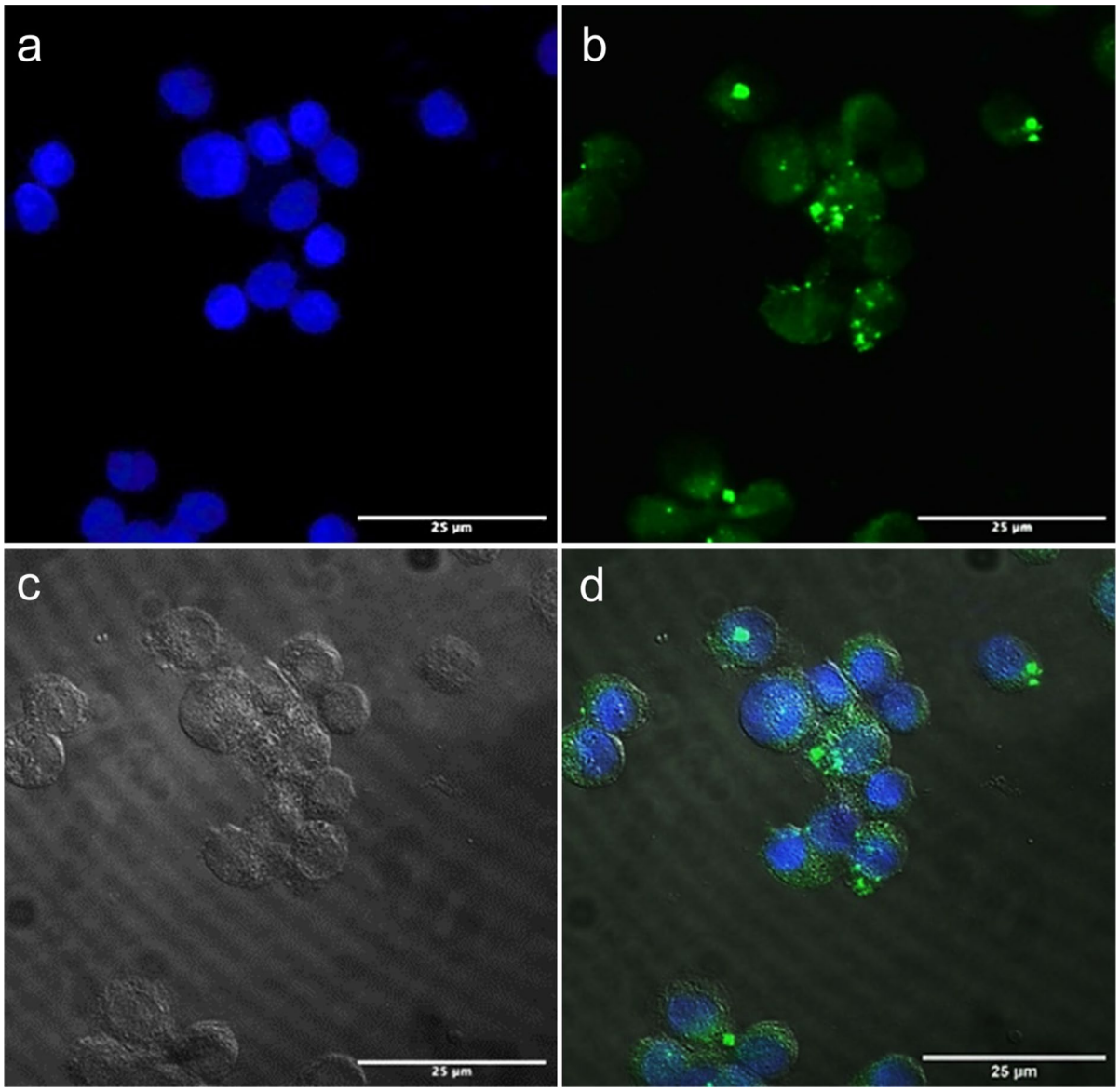


**Fig. 8** Uptake of BCmFs containing fluorescently labelled BSA (BCmFs-BSA-FITC). Confocal microscopy images of U937 macrophage cells after incubation with BCmFs-BSA-FITC **a** Blue nucleus image with DAPI filter, **b** internalized FITC-BSA from BCmFs appeared green in colour, **c** cell images with white light, **d** merged images obtained with all filters, BCmFs-BSA-FITC appearance determined to be localized around the nucleus

et al. 2011; Martínez-Sanz et al. 2011; Zaborowska et al. 2010). It has been known that physicochemical properties such as size, hydrophobicity, surface charge, shape, and composition of the adjuvants play an essential role in the adjuvant effect (Bastola and Lee 2019; Kreuter and Haenzel 1978). Apart from other physicochemical properties, the water-insoluble adjuvants have a higher cellular uptake, thus triggering a higher immune response (Woodard 1989).

One of the properties of BC is that it is in the form of water-insoluble microfibrils, which makes it a good candidate for vaccine adjuvant. However, there is no studies investigating the vaccine adjuvant potential of BC. Hydrolysis processes on cellulose samples are carried out with sulfuric acid, which causes the

amorphous areas of the material to break into fibrils by controlled hydrolysis. Although plant-derived cellulose and BC have the same chemical structure, they have different structural and mechanical properties. BC shows a thinner fibril structure, higher water-holding capacity, and higher crystallinity (Iguchi et al. 2000; Wan et al. 2009). In addition, plant-derived cellulose is combined with lignin and hemicellulose structures, while BC has a chemically pure structure. In our study, after the hydrolysis process, it was observed that microfibrils of similar size were obtained by hydrolysis with 2.5 M $H_2SO_4$ similar with the study by De Oliveira et al. (2011).

SEM images and analysis showed that after hydrolysis, the BC fibrils were 0.57–4.072–8 μm in size and needle-shaped (Fig. 3d). It is known that needle-like particles can result in inflammasomes activation and thus better induce immune response compare with spherical particles (Donaldson et al. 2010). Among needle-like particles, larger particles with micrometre size are typically more capable of activating inflammasomes (Caicedo et al. 2013).

The physical absorption of the antigen has advantages compared to other conjugation procedures. However, the conjugation method may cause modification of peptide epitope in addition to complications regarding the reproducibility of conjugate structures (Kazzaz et al. 2000; Singh et al. 2004). Due to BC's high water absorption capacity, a simple mixing method was used, frequently used in polymer adjuvants as a conjugation method (Kreuter et al. 1988). The spectrum of the BCmFs-BSA conjugate in the protein-specific amide-I and amide-II bands (Guo et al. 2019) and associated with the cellulose chain backbone (Abderrahim et al. 2015) is an indication that the conjugate contains both cellulose and model antigen (Fig. 4).

The immunostimulatory effects of the BCmFs-BSA conjugates were measured with TNF-α and IL-6 ELISA kit on the U937 human macrophage cell line. Conjugates containing different BSA concentrations (500, 250, and 100 μg/ml) were administered to cells, and all were found to induce TNF-α secretion in cells. When TNF-α levels were examined, while there was no significant difference between the sample containing BCmFs and the negative control, BCmFs-BSA conjugate had significantly higher (3,7 times) TNF-α level than BSA alone. Furthermore, the BCmFs-BSA conjugate had a higher (1.78 times) TNF-α level than the alum-BSA conjugate (Fig. 7a). The reason for the higher TNF-α secretion induced by BCmFs in comparison to the alum group containing the same amount of BSA is thought to be due to the higher cellular uptake. Physicochemical properties of particles such as size and shape (Zheng and Yu 2016), surface charge (He et al. 2010), surface hydrophobicity/hydrophilicity (Kreuter et al. 1988) and solubility/insolubility (Woodard 1989) directly affect the cellular uptake mechanism. Studies have shown that filamentous particles with a higher aspect ratio have a higher cellular uptake potential than spherical particles of the same size (Dasgupta et al. 2014). The limited number of binding sites of spherical particles allows limited interaction with target cell receptors, while filamentous particles have a higher surface area that facilitates their interaction with the cell surface; thus, filamentous, elongated particles are more effective in adhesion to cells than spherical particles (Agarwal et al. 2013). Woodard et al. have shown that water-insoluble molecules induce a higher immune response by increasing cellular uptake (Woodard 1989). Due to the higher aspect ratio and filamentous structure of BCmFs compared to alum adjuvant, it was thought that the higher cellular uptake and, thus, higher TNF-α level was achieved.

Depending on their mode of action, adjuvants are used to stimulate the Th1 and/or Th2-mediated immune response. The production of IL-2, TNF- α, and IFN-γ are characteristics of the Th1 immune response mediated by Th1 cells. In addition, the production of cytotoxic T lymphocytes (CTL) and cell-mediated inflammatory reactions requires a Th1 immune response. Th2 cells are characterized by the secretion of IL-4, IL-5, IL-6, IL-10, and IL-13 cytokines, which regulate B cell activation and antibody production. While the Th1 response is essential for protective immunity against intracellular pathogens, including viruses, bacteria, and protozoa, and against cancer cells, Th2 immunity is effective for defence against most bacteria as well as against some viral infections (Cox and Coulter 1997). The most commonly used adjuvants, such as alum, stimulate the Th2 immune response and is ineffective against intracellular pathogens. Studies have shown that IL-6 secretion supports Th2 differentiation and inhibits Th1 polarization and IFN-γ production by inducing the expression of IL-4 during the activation of CD4 + T cells (Diehl and Rincón 2002). When IL-6

levels were examined in this study, no statistically significant results were obtained between the groups except the positive control group (LPS). It was shown that the BCmFs did not induce the IL-6 production and appeared to induce the Th1 immune response (Fig. 7b). In this study, BC microfibrils were shown to be phagocytosed by macrophage cells and increased cellular uptake of the target antigen (Fig. 8).

In conclusion, increased TNF-α cytokine levels with restricted IL-6 production demonstrated that BCmFs enhanced the immune response to the antigen BSA. It is also desirable for a vaccine adjuvant that BC, when administered alone, does not stimulate macrophages. Due to these properties, it has been determined that BC has the potential to be an adjuvant that can increase the immunogenicity of vaccine antigens that do not activate the immune system or that have weak immunogenic properties. These results are the first to report that BCmFs have the potential to be an alternative to alum adjuvants.

**Acknowledgments** The authors thank Professor Kemal S. Korkmaz for his support in cytokine release experiments.

**Authors' contributions** All authors contributed to the study's conception and design. Formal analysis and investigation: ÖS, Data collection and analysis: ÖS and AG, Writing-first draft preparation: ÖS and AG, Writing-review and editing: EEH, Supervision: EEH.

**Funding** This project was funded by The Scientific Research Foundation of Ege University (Project Number: 20783).

**Declarations**

**Conflict of interest** There are no conflicts to declare.

**Ethics approval and consent to participate** Not applicable.

**Consent for publication** All of the material is owned by the authors and/or no permissions are required.

**Availability of data and materials** Data used and/or analyzed during the study are available from the corresponding author upon reasonable request.

## References

Abderrahim B, Abderrahman E, Mohamed A, Fatima T, Abdesselam T, Krim O (2015) Kinetic thermal degradation of cellulose, polybutylene succinate and a green composite: comparative study. World J Environ Eng 3(4):95–110. https://doi.org/10.12691/WJEE-3-4-1

Agarwal R, Singh V, Jurney P, Shi L, Sreenivasan SV, Roy K (2013) Mammalian cells preferentially internalize hydrogel nanodiscs over nanorods and use shape-specific uptake mechanisms. Proc Natl Acad Sci USA 110(43):17247–17252. https://doi.org/10.1073/pnas.1305000110

Aguilar JC, Rodríguez EG (2007) Vaccine adjuvants revisited. Vaccine 25(19):3752–3762. https://doi.org/10.1016/j.vaccine.2007.01.111

Bastola R, Lee S (2019) Physicochemical properties of particulate vaccine adjuvants: their pivotal role in modulating immune responses. J Pharm Investig 49(3):279–285. https://doi.org/10.1007/s40005-018-0406-4

Bauer C, Duewell P, Mayer C, Lehr HA, Fitzgerald KA, Dauer M, Tschopp J, Endres S, Latz E, Schnurr M (2010) Colitis induced in mice with dextran sulfate sodium (DSS) is mediated by the NLRP3 inflammasome. Gut 59(9):1192–1199. https://doi.org/10.1136/gut.2009.197822

Bilgi E, Bayir E, Sendemir-Urkmez A, Hames EE (2016) Optimization of bacterial cellulose production by *Gluconacetobacter xylinus* using carob and haricot bean. Int J Biol Macromol 90:2–10. https://doi.org/10.1016/j.ijbiomac.2016.02.052

Bradford MM (1976) A rapid and sensitive method for the quantitation of microgram quantities of protein utilizing the principle of protein-dye binding. Anal Biochem 72:248–254. https://doi.org/10.1016/j.cj.2017.04.003

Caicedo MS, Samelko L, McAllister K, Jacobs JJ, Hallab NJ (2013) Increasing both CoCrMo-alloy particle size and surface irregularity induces increased macrophage inflammasome activation in vitro potentially through lysosomal destabilization mechanisms. J Orthop Res 31(10):1633–1642. https://doi.org/10.1002/jor.22411

Calabro S, Tritto E, Pezzotti A, Taccone M, Muzzi A, Bertholet S, Gregorio ED, Hagan DTO, Baudner B, Seubert A (2013) The adjuvant effect of MF59 is due to the oil-in-water emulsion formulation, none of the individual components induce a comparable adjuvant effect. Vaccine 31(33):3363–3369. https://doi.org/10.1016/j.vaccine.2013.05.007

Cooper PD, Petrovsky N (2011) Delta inulin: a novel, immunologically active, stable packing structure comprising β-D-[2 → 1] poly(fructo-furanosyl) αd-glucose polymers. Glycobiology 21(5):595–606. https://doi.org/10.1093/glycob/cwq201

Cox JC, Coulter AR (1997) Adjuvants—a classification and review of their modes of action. Vaccine 15(3):248–256. https://doi.org/10.1016/S0264-410X(96)00183-1

Dasgupta S, Auth T, Gompper G (2014) Shape and orientation matter for the cellular uptake of nonspherical particles. Nano Lett 14(2):687–693. https://doi.org/10.1021/nl403949h

De Oliveira RL, Da Silva Barud H, De Assunção RMN, Da Silva Meireles C, Carvalho GO, Filho GR, Messaddeq Y, Ribeiro SJL (2011) Synthesis and characterization of microcrystalline cellulose produced from bacterial cellulose. J Therm Anal Calorim 106(3):703–709. https://doi.org/10.1007/s10973-011-1449-1

Debelec-Butuner B, Alapinar C, Varisli L, Erbaykent-Tepedelen B, Hamid SM, Gonen-Korkmaz C, Korkmaz KS (2014) Inflammation-mediated abrogation of androgen signaling: an *in vitro* model of prostate cell inflammation.

Mol Carcinog 53(2):85–97. https://doi.org/10.1002/mc.21948

Del Giudice G, Rappuoli R, Didierlaurent AM (2018) Correlates of adjuvanticity: a review on adjuvants in licensed vaccines. Semin Immunol 39(May):14–21. https://doi.org/10.1016/j.smim.2018.05.001

Devy J, Balasse E, Kaplan H, Madoulet C, Andry MC (2006) Hydroxyethylstarch microcapsules: a preliminary study for tumor immunotherapy application. Int J Pharm 307(2):194–200. https://doi.org/10.1016/j.ijpharm.2005.09.035

Diehl S, Rincón M (2002) The two faces of IL-6 on Th1 / Th2 differentiation. Mol Immunol 39:531–536. https://doi.org/10.1016/S0161-5890(02)00210-9

Donaldson K, Murphy FA, Duffin R, Poland CA (2010) Asbestos, carbon nanotubes and the pleural mesothelium: a review of the hypothesis regarding the role of long fibre retention in the parietal pleura, inflammation and mesothelioma. Part Fibre Toxicol. https://doi.org/10.1186/1743-8977-7-5

Guo C, Guo X, Chu W, Jiang N, Li H (2019) Spectroscopic study of conformation changes of bovine serum albumin in aqueous environment. Chin Chem Lett 30(6):1302–1306. https://doi.org/10.1016/j.cclet.2019.02.023

He C, Hu Y, Yin L, Tang C, Yin C (2010) Effects of particle size and surface charge on cellular uptake and biodistribution of polymeric nanoparticles. Biomaterials 31(13):3657–3666. https://doi.org/10.1016/j.biomaterials.2010.01.065

Hestrin S, Schramm M (1954) Synthesis of cellulose by *Acetobacter xylinum*. 2. Preparation of freeze-dried cells capable of polymerizing glucose to cellulose. Biochem J 58(2):345–352. https://doi.org/10.1042/bj0580345

Iguchi M, Yamanaka S, Budhiono A (2000) Bacterial cellulose—a masterpiece of nature's arts. J Mater Sci 35(2):261–270. https://doi.org/10.1023/A:1004775229149

Kalam MA, Khan AA, Alshamsan A (2017) Non-invasive administration of biodegradable nano-carrier vaccines. Am J Transl Res 9(1):15–35

Kanchan V, Panda AK (2007) Interactions of antigen-loaded polylactide particles with macrophages and their correlation with the immune response. Biomaterials 28(35):5344–5357. https://doi.org/10.1016/j.biomaterials.2007.08.015

Kazzaz J, Neidleman J, Singh M, Ott G, O'Hagan DT (2000) Novel anionic microparticles are a potent adjuvant for the induction of cytotoxic T lymphocytes against recombinant p55 gag from HIV-1. J Control Release 67(2–3):347–356. https://doi.org/10.1016/S0168-3659(00)00226-1

Keskin Z, Sendemir Urkmez A, Hames EE (2017) Novel keratin modified bacterial cellulose nanocomposite production and characterization for skin tissue engineering. Mater Sci Eng C Mater Biol Appl 75:1144–1153. https://doi.org/10.1016/j.msec.2017.03.035

Kreuter J, Haenzel I (1978) Mode of action of immunological adjuvants: some physicochemical factors influencing the effectivity of polyacrylic adjuvants. Infect Immun 19(2):667–675. https://doi.org/10.1128/iai.19.2.667-675.1978

Kreuter J, Liehl E, Berg U, Soliva M, Speiser PP (1988) Influence of hydrophobicity on the adjuvant effect of particulate polymeric adjuvants. Vaccine 6(3):253–256. https://doi.org/10.1016/0264-410X(88)90220-4

Lunardi CN, Gomes AJ, Rocha FS, De Tommaso J, Patience GS (2021) Experimental methods in chemical engineering: Zeta potential. Can J Chem Eng 99(3):627–639. https://doi.org/10.1002/cjce.23914

Martínez-Sanz M, Lopez-Rubio A, Lagaron JM (2011) Optimization of the nanofabrication by acid hydrolysis of bacterial cellulose nanowhiskers. Carbohydr Polym 85(1):228–236. https://doi.org/10.1016/j.carbpol.2011.02.021

Mchugh KJ, Guarecuco R, Langer R, Jaklenec A (2015) Single-injection vaccines : Progress, challenges, and opportunities. J Control Release 219:596–609. https://doi.org/10.1016/j.jconrel.2015.07.029

Mohd Amin MCI, Ahmad N, Pandey M, Jue Xin C (2014) Stimuli-responsive bacterial cellulose-g-poly(acrylic acid-co-acrylamide) hydrogels for oral controlled release drug delivery. Drug Dev Ind Pharm 40(10):1340–1349. https://doi.org/10.3109/03639045.2013.819882

Mosmann T (1983) Rapid colorimetric assay for cellular growth and survival: application to proliferation and cytotoxicity assays. J Immunol Methods 65:55–63. https://doi.org/10.1039/c6ra17788c

Müller A, Indrajeet S, Khushboo M, Gauri K, Sen DJ (2011) Hydrotropy: a promising tool for solubility enhancement: a review. Int J Drug Dev Res 3(2):26–33. https://doi.org/10.1002/jps

Mustafaev M (2004) Functionally biopolymer systems. Sigma 4:1–200

Nanishi E, Dowling DJ, Levy O (2020) Toward precision adjuvants: Optimizing science and safety. Curr Opin Pediatr 32(1):125–138. https://doi.org/10.1097/MOP.0000000000000868

Niikura K, Matsunaga T, Suzuki T, Kobayashi S, Yamaguchi H, Orba Y, Kawaguchi A, Hasegawa H, Kajino K, Ninomiya T, Ijiro K, Sawa H (2013) Gold nanoparticles as a vaccine platform: influence of size and shape on immunological responses in vitro and in vivo. ACS Nano 7(5):3926–3938. https://doi.org/10.1021/nn3057005

Oz YE, Keskin-Erdogan Z, Safa N, Hames Tuna EE (2021) A review of functionalised bacterial cellulose for targeted biomedical fields. J Biomater Appl 36(4):648–681. https://doi.org/10.1177/0885328221998033

Pertile RAN, Andrade FK, Alves C, Gama M (2010) Surface modification of bacterial cellulose by nitrogen-containing plasma for improved interaction with cells. Carbohydr Polym 82(3):692–698. https://doi.org/10.1016/j.carbpol.2010.05.037

Petrovsky N, Aguilar JC (2004) Vaccine adjuvants: current state and future trends. Immunol Cell Biol 82:488–496. https://doi.org/10.1111/j.1440-1711.2004.01272.x

Piatkowski A, Drummer N, Andriessen A, Ulrich D, Pallua N (2011) Randomized controlled single center study comparing a polyhexanide containing bio-cellulose dressing with silver sulfadiazine cream in partial-thickness dermal burns. Burns 37(5):800–804. https://doi.org/10.1016/j.burns.2011.01.027

Plotkin S (2014) History of vaccination. Proc Nat Acad Sci USA 111(34):12283–12287. https://doi.org/10.1073/pnas.1400472111

Provder T (1997) Challenges in particle size distribution measurement past, present and for the 21st century. Prog Org Coat 32(1–4):143–153. https://doi.org/10.1016/S0300-9440(97)00043-X

Seth A, Heo MB, Sung MH, Lim YT (2015) Infection-mimicking poly(γ-glutamic acid) as adjuvant material for effective anti-tumor immune response. Int J Biol Macromol 75:495–504. https://doi.org/10.1016/j.ijbiomac.2015.02.013

Sheng KC, Pouniotis DS, Wright MD, Tang CK, Lazoura E, Pietersz GA, Apostolopoulos V (2006) Mannan derivatives induce phenotypic and functional maturation of mouse dendritic cells. Immunology 118(3):372–383. https://doi.org/10.1111/j.1365-2567.2006.02384.x

Singh M, Kazzaz J, Ugozzoli M, Chesko J, O'Hagan DT (2004) Charged polylactide co-glycolide microparticles as antigen delivery systems. Expert Opin Biol Ther 4(4):483–491. https://doi.org/10.1517/14712598.4.4.483

Vannucci L, Šíma P, Vetvicka V, Křižan J (2017) Lentinan properties in anticancer therapy: a review on the last 12-year literature. Am J Immunol 13(1):50–61. https://doi.org/10.3844/ajisp.2017.50.61

Vasiliev YM (2014) Chitosan-based vaccine adjuvants: Incomplete characterization complicates preclinical and clinical evaluation. Expert Rev Vaccines 14(1):37–53. https://doi.org/10.1586/14760584.2015.956729

Wan YZ, Luo H, He F, Liang H, Huang Y, Li XL (2009) Mechanical, moisture absorption, and biodegradation behaviours of bacterial cellulose fibre-reinforced starch biocomposites. Compos Sci Technol 69(7–8):1212–1217. https://doi.org/10.1016/j.compscitech.2009.02.024

Wang X, Uto T, Akagi T, Akashi M, Baba M (2010) A clinically relevant, syngeneic model of spontaneous, highly metastatic B16 mouse melanoma. Anticancer Res 30(12):4799–4804. https://doi.org/10.1002/jmv

Woodard L (1989) Adjuvant activity of water-insoluble surfactants. Lab Anim Sci 39(3):222–225

Yang JZ, Yu JW, Sun DP, Yang XJ (2010) Preparation of novel Ag/bacterial cellulose hybrid nanofibers for antimicrobial wound dressing. Adv Mater Res 152–153:1771–1774. https://doi.org/10.4028/www.scientific.net/AMR.152-153.1771

Zaborowska M, Bodin A, Bäckdahl H, Popp J, Goldstein A, Gatenholm P (2010) Microporous bacterial cellulose as a potential scaffold for bone regeneration. Acta Biomater 6(7):2540–2547. https://doi.org/10.1016/j.actbio.2010.01.004

Zhang N, Zheng BJ, Lu L, Zhou Y, Jiang S, Du L (2015) Advancements in the development of subunit influenza vaccines. Microbes Infect 17(2):123–134. https://doi.org/10.1016/j.micinf.2014.12.006

Zheng M, Yu J (2016) The effect of particle shape and size on cellular uptake. Drug Deliv Transl Res 6(1):67–72. https://doi.org/10.1007/s13346-015-0270-y